Shakedown of a Plate with a Circular Hole - an educational problem

Journal Title
XX(X):1–11

DOI: 10.1177/ToBeAssigned
www.sagepub.com/
SAGE

Yifeng Chen[1] and David A. Hills[1]

Abstract

The shakedown limit for an infinite plate containing a circular hole and subject to oscillatory arbitrary remote loading is found, first by using Melan's lower bound theorem, and secondly by using a finite element model. It is shown that in some cases the limit found from the Melan theorem using the solution for the residual state of stress for an over-pressurised hole provides the exact solution, specifically when the limiting factor is the reversal of the state of stress at a particular point, while in other cases the shakedown limit is rather higher.

Keywords

Melan's theorem, Kirsch's solution, Shakedown limit, Elastic shakedown, Residual stress

Introduction

The method of shakedown analysis came into existence in the 1930s, first developed by Bleich[1] and Melan[2], which provided a conservative lower bound to the actual shakedown limit. Later on, Koiter[3] supplied the basic concepts and determined an upper bound limit by using compatibility considerations. The fundamentals of the shakedown analysis for the engineering structure are well explained in König[4]. Mackenzie *et al.*[5] has further reviewed the elastic compensation method for elastic shakedown analysis, which concerntrated on finite element implementation.

Today, Civil Engineering design codes for structural steelwork now invariably centre on plastic design rules, which makes better use of material than elastic procedures, and implicit in those codes is the process of the shakedown. Most of the existing algorithms used for shakedown analysis in Civil Engineering were evaluated by Fuschi, Pisano and Weichert[6]. Although shakedown in skeletal frames is widely studied and understood, the application of shakedown principles to continuum problems is not usually treated in undergraduate courses and, indeed, there is little detail in textbooks on the process of the shakedown.

The shakedown analysis of a plate with a circular hole, shown in Figure 1, has been previously discussed by Muscat *et al.*[7]. This work applied the lower bound theorem developed by Polizzotto[8], in which the applied load is decomposed to the steady state and cyclic load, and the shakedown limit will be the superposition of the responses of those two types of load. Notice that in the shakedown limit calculation of the method mentioned in Muscat *et al.*, the inelastic stress field resulted by the steady state load is required. Because the inelastic response in most case is not analytically feasible, hence finite element analysis is usually involved in Possi's theorem calculation.

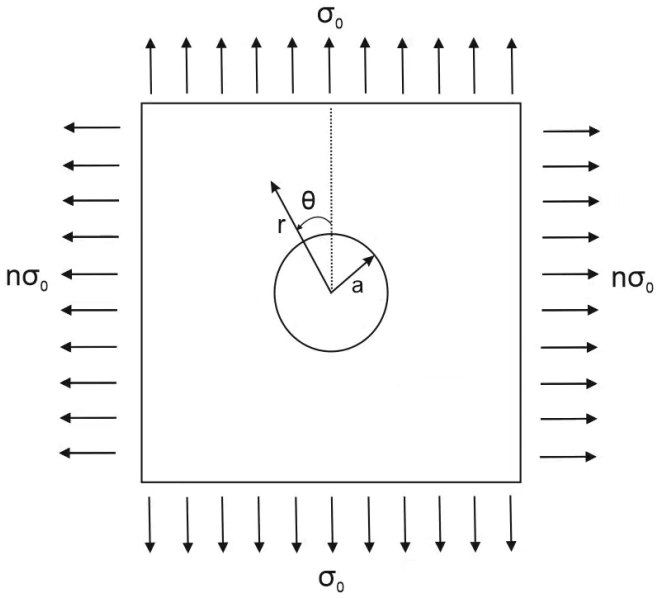

Figure 1. Geometry of a plate with a circular hole problem.

In this paper, we will analyze the shakedown problem of a plate with a circular hole again, but the object of this paper is to provide a simple, practical illustration of the application of the lower bound theorem, due to Melan[9], and to investigate the strength of the problem generally. Melan's theorem may be stated as follows " If *some* residual state of stress may be found which, together with the applied stresses, results in an elastic state of stress everywhere and at all points in the loading cycle, the system will shake down in a finite number

[1]Department of Engineering Science, University of Oxford, Parks Road, OX1 3PJ Oxford, United Kingdom

Corresponding author:
David Hills, *Tel.*: +44 1865 273811
Email: David.Hills@eng.ox.ac.uk

of cycles at at least the load assumed". The important thing is that we do not have to speculate what the exact form of the residual stress state is - that may be tricky - but only some self consistent residual stress state which satisfies all free boundary conditions.

Formulation

The plate is subject to a general remote state of stress, Figure 1. We align the polar axis set with one of the principal directions ($\theta = 0$ with σ_0) and the other principal remote stress is given by $n\sigma_0$, where $-1 < n < 1$. The state of stress within the plate is a classical problem usually solved using an Airy stress function, and with the result[10].

$$\left\{ \begin{array}{c} \sigma_{rr} \\ \sigma_{\theta\theta} \\ \sigma_{r\theta} \end{array} \right\} = \frac{1}{2}\sigma_0 \left\{ \begin{array}{c} 1 - \frac{a^2}{r^2} + \cos 2\theta \left(\frac{3a^4}{r^4} - \frac{4a^2}{r^2} + 1 \right) \\ 1 + \frac{a^2}{r^2} - \cos 2\theta \left(\frac{3a^4}{r^4} + 1 \right) \\ \sin 2\theta \left(\frac{3a^4}{r^4} - \frac{2a^2}{r^2} - 1 \right) \end{array} \right\} + \frac{n}{2}\sigma_0 \left\{ \begin{array}{c} 1 - \frac{a^2}{r^2} - \cos 2\theta \left(\frac{3a^4}{r^4} - \frac{4a^2}{r^2} + 1 \right) \\ 1 + \frac{a^2}{r^2} + \cos 2\theta \left(\frac{3a^4}{r^4} + 1 \right) \\ -\sin 2\theta \left(\frac{3a^4}{r^4} - \frac{2a^2}{r^2} - 1 \right) \end{array} \right\}, \tag{1}$$

where a is the radius of the hole. The severest state of stress lies at the surface of the hole, where the tractions vanish, and the remaining stress component is given by

$$\sigma_{\theta\theta}(a, \theta) = \sigma_0 (1 + n) - 2\sigma_0 (1 - n) \cos 2\theta. \tag{2}$$

If we assume a state of plane stress, and that the material from which the plate is made satisfies a Von Mises yield condition, with a yield stress in pure shear k, the elastic limit is attained when

$$\sigma_{\theta\theta}^2 = 3k^2. \tag{3}$$

The exact points of the maximum and minimum values of $\sigma_{\theta\theta}$ at the edge of the hole are found by taking the derivative of equation (2) with respect to θ, and the maximum value ($\theta = \pi/2$) and the minimum value ($\theta = 0$) are:

$$\sigma_{\theta\theta}(a, \pi/2) = \sigma_0 (3 - n) \tag{4}$$

$$\sigma_{\theta\theta}(a, 0) = \sigma_0 (3n - 1). \tag{5}$$

The elastic limit for the problem is therefore found by substituting equation (4) into equation (3) and, in particular is given by $\sigma_0/k = \sqrt{3}/4$ ($n = -1$, pure shear), $\sigma_0/k = \sqrt{3}/3$($n = 0$, uniaxial tension), or $\sigma_0/k = \sqrt{3}/2$ ($n = 1$, cylindrical state of remote load). The general elastic limit is given by $\sigma_0/k = \sqrt{3}/(3 - n)$. Thus result are included in Figure 2(a) as the yellow line (all other lines in figure 2(a) will be introduced in later sections).

Residual Stress Field

Clearly, except in the case when $n = 1$, the problem is not axi-symmetric, and neither the state of stress produced by the applied load nor any self-generated residual stress field will be symmetrical, but it is difficult to speculate on the form of the residual stress state in the general case, and even more difficult to form a potential solution to use. We therefore choose a very simple res idual stress field, one which is axi-symmetric, and formed by the over-pressurization of the plate with a hole, followed by relaxation. The axi-symmetric solution has only one non-zero displacement, in the radial direction, and it is straightforward to solve for the state of stress after relaxation. This is a just a special case of the elastic-plastic analysis of thick-walled cylinder, when the outer radius is permitted to be infinitely big. After pressurization to a value of $p_0/k = \eta$ (and $1 < \eta < \frac{2+\sqrt{3}}{2}$), the residual stress state left is given by, for $r \leqslant r_p$:

$$\sigma_{rr}^{res}(r)/k = 2\left(\ln\left(\frac{r}{a}\right)\right) - \eta\left(1 - \frac{a^2}{r^2}\right) \tag{6}$$

$$\sigma_{\theta\theta}^{res}(r)/k = 2\left(\ln\left(\frac{r}{a}\right) + 1\right) - \eta\left(1 + \frac{a^2}{r^2}\right) \tag{7}$$

and for $r > r_p$:

$$\sigma_{rr}^{res}(r)/k = -\left(\frac{r_p}{r}\right)^2 + \eta\left(\frac{a}{r}\right)^2 \tag{8}$$

$$\sigma_{\theta\theta}^{res}(r)/k = \left(\frac{r_p}{r}\right)^2 - \eta\left(\frac{a}{r}\right)^2 \tag{9}$$

where

$$r_p = a\left(2 - \sqrt{2 - \eta}\right) \tag{10}$$

The residual stresses are plotted in Figure 3(a) ($\sigma_{rr}^{res}(r)$) and Figure 3(b) ($\sigma_{\theta\theta}^{res}(r)$). Note that if $\eta > \frac{2+\sqrt{3}}{2}$ upon relaxation there is secondary plastic flow, and we have not considered this case in detail.

Load-unload Case Analysis

Application of Melan's Theorem

It is important to note that Melan's theorem requires *all* points within the body to be within the elastic limit during the loading cycle for shakedown to be achieved, and therefore a full-field calculation is needed. But we may speculate what the optimum value of the residual stress field is by looking at **the edge of the hole**, where the severest state of stress occurs, and a picture will emerge. We shall now take a simple load-unload case where load varies between zero and σ_0 as an example to illustrate how we find the shakedown limit by finding the optimal residual stress at the edge of the hole using Melan's theorem (the residual stress fields then can be generated using equations (6)-(10) by matching $\sigma_{\theta\theta}(a)$ with the optimal residual stress we proposed at the edge of the hole). Additionally, the comparisons between the lower bound shakedown limits with the actual shakedown limits found by Finite Element Analysis (FEA) are also evaluated.

First, if we think of the problem of uniaxial tension applied to the plate ($n = 0$) we see from equations (4) and (5) that if residual stress has not been considered, point $(a, 0)$, where $\sigma_{\theta\theta}(a, \pi/2)/\sigma_0 = -1$, and point $(a, \pi/2)$, where $\sigma_{\theta\theta}(a, \pi/2)/\sigma_0 = 3$ have severe states of stress of opposite sign. So, if the magnitude of the axi-symmetric residual stress field on the edge of the hole is $\sigma_{\theta\theta}^{res}(a)/\sigma_0 = A$, the optimal choice of A is when

$$-1 + A = -(3 + A)$$

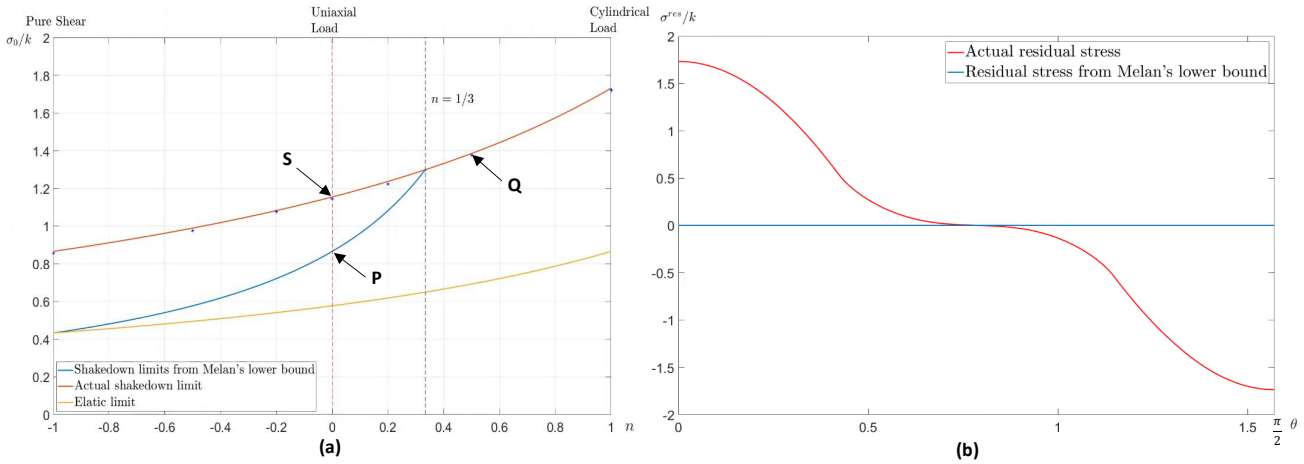

Figure 2. (a) Comparison between the elastic limit, actual shakedown limit and shakedown limit calculated by Melan's lower bound for the load-unload case. (b) For $n = -1$, comparison between the actual residual stress field at the edge of the hole, when the applied load reaches the actual shakedown limit $\sigma_0/k = \sqrt{3}/2$, and that implied by Melan's theorem when the lower bound shakedown limits $\sigma_0/k = \sqrt{3}/4$ applied.

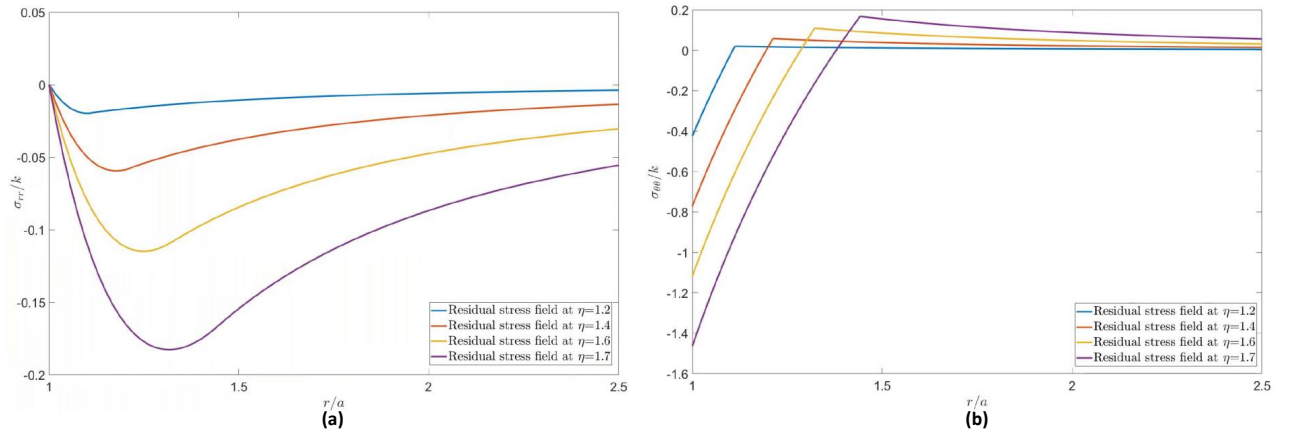

Figure 3. Residual stress (a) $\sigma^{res}_{\theta\theta}(r)$, (b) $\sigma^{res}_{\theta\theta}(r)$, generated by internal pressure η.

or $\sigma^{res}_{\theta\theta}(a)/\sigma_0 = -1$. According to Melan's theorem, the lower bound of the shakedown limit λ is therefore given by

$$\begin{aligned}\sigma_{\theta\theta}\,(a,\pi/2) + \sigma^{res}_{\theta\theta}(a) &= -(\sigma_{\theta\theta}(a,0) + \sigma^{res}_{\theta\theta}(a)) \\ &= 2\sigma_0 = 2\lambda k = \sqrt{3}k,\end{aligned}$$

or $\lambda = \sigma_0/k = \sqrt{3}/2$, i.e., a 50% increase on the elastic limit. When the applied load is removed fully the residual stress around the hole alone remains, but we know that that it is half the magnitude of the state of stress at the critical points in the presence of the load, so that there is no possibility of the component entering the plastic state because of the residual stress alone.

Secondly, if we think about a state of remote applied pure shear ($n = -1$), again from equations (4)-(5), we see that $\sigma_{\theta\theta}(a,0) = -\sigma_{\theta\theta}(a,\pi/2)$, so that no residual stress *of the character being considered* can help, and so we expect the shakedown limit to be the same as the elastic limit, by the theorem.

When we have a cylindrical applied remote stress ($n = 1$), everywhere around the edge of the hole experiences a stress given by $\sigma_{\theta\theta}\,(a,\theta) = 2\sigma_0$ if residual stress has not been considered. The optimal choice of residual stress is therefore one which leads to incipient forwards slip when the maximum external load is applied and incipient reverse slip when the external load is removed, i.e., in the optimal case:

$$2\sigma_0 + \sigma^{res}_{\theta\theta}(a) = -\sigma^{res}_{\theta\theta}(a) = \sqrt{3}k.$$

the implied shakedown limit is given by $\lambda = \sigma_0/k = \sqrt{3}$, i.e. twice the elastic limit. Because the whole solution is axi-symmetrical, we might look forward to the actual shakedown limit being the same as that implied by the lower bound.

We extend the above reasoning to the entire range of n, [-1,1], bearing in mind that there are two key controlling points in the physical space, $(a,0)$ and $(a,\pi/2)$, to consider. In general, the net state of stress of those two points for the applied load σ_0 is displayed in Table 1. Also bear in mind that the residual stress itself may not to exceed the elastic limit, $\pm\sqrt{3}k$, to avoid any secondary plastic flow. When $-1 \leq n \leq 1/3$, which includes both the uniaxial and pure shear loading cases, from equation (5), the most negative stress arose at $(a,0)$. Contribution from the applied stress

together with the residual stress must not exceed the elastic limit in the reverse direction. As a result, the two extreme points during loading cycle are located at $(a,0)$ and $(a,\pi/2)$. The residual stress at the edge of the hole, therefore, needs to satisfy:

$$\sigma_{\theta\theta}\,(a,\pi/2)+\sigma_{\theta\theta}^{res}(a)=-(\sigma_{\theta\theta}(a,0)+\sigma_{\theta\theta}^{res}(a))=\sqrt{3}k,$$

and hence, by substituting $\sigma_{\theta\theta}$ with equation (4) and (5), we have

$$\sigma_{\theta\theta}^{res}(a)=\frac{-\sqrt{3}(1+n)k}{2-2n} \tag{11}$$

$$\lambda=\sigma_0/k=\frac{\sqrt{3}}{2-2n}\quad -1\le n\le 1/3 \tag{12}$$

The shakedown limit λ determined using Melan's theorem, for $-1\le n<1/3$, are plotted in Figure 2(a) as the blue line.

Table 1. Values of net stress $\sigma_{\theta\theta}(a,\theta)$ at $\theta=0$ and $\theta=\pi/2$ for the applied load σ_0.

$\theta=0$	$\theta=\pi/2$
$\sigma_0(3n-1)+\sigma_{\theta\theta}^{res}(a)$	$\sigma_0(3-n)+\sigma_{\theta\theta}^{res}(a)$

The illustrations of Melan's theorem may also be displayed by looking at trajectories in the deviatoric plane. The deviatoric yielding surface is a circle centred at the origin with radius $\sqrt{2}k$, and the projection of any stress σ to a deviatoric plane with a Cartesian coordinate system is transformed by the following equations:

$$|\sigma|_x=\sigma\cdot\frac{1}{\sqrt{2}}\begin{bmatrix}0\\-1\\1\end{bmatrix},\quad |\sigma|_y=\sigma\cdot\frac{1}{\sqrt{6}}\begin{bmatrix}2\\-1\\-1\end{bmatrix},$$

Where $|\sigma|_x$ and $|\sigma|_y$ represent the x and y values of the stress σ on the deviatoric plane. We also represent the magnitude of any stress σ on the deviatoric plane as $|\sigma|_e$, so

$$|\sigma|_e=\sqrt{|\sigma|_x^2+|\sigma|_y^2}.$$

Taking $n=0$ as an example, when the plate is loaded under the shakedown limit deduced by Melan's theorem (point P in the Figure 2(a)), the magnitude of the elastic stress and axi-symmetrical residual stress at two controlling points on the deviatoric plane is shown in Table 2.
Therefore, for the case $n=0$, by applying Melan's theorem, the deviatoric stress trajectories of the two controlling points for a load-unload cycle when the plate is loaded under the lower bound shakedown limit, are shown in Figure 4(a.1).

Next, in the case of $1/3<n\le 1$, positive stress arose at $(a,0)$, then the magnitude of the residual stress is no longer restricted. In other words, the residual stress at the edge of the hole can be as small as the elastic limit in the reverse direction. Therefore, considering the critical point with maximum elastis stress, we have

$$\sigma_{\theta\theta}\,(a,\pi/2)+\sigma_{\theta\theta}^{res}(a)=\sigma_0(3-n)-\sqrt{3}k=\sqrt{3}k,$$

hence the shakedown limits:

$$\lambda=\frac{2\sqrt{3}}{3-n}\quad 1/3<n\le 1 \tag{13}$$

which has been plotted in Figure 2(a) as the red line on the right-hand side of the line "$n=1/3$". In this case, the two extremes of the loading cycle are located at the same point $(a,\pi/2)$, occurring at both the maximum applied load and the unload state. The same as above, for $1/3<n\le 1$, Melan's theorem can be further demonstrated by the trajectories in the deviatoric plane. Taking $n=0.5$ as an example, when the plate is loaded under the shakedown limit determined by Melan's theorem (point Q in Figure 2(a)), the magnitude of the relevant stress on the deviatoric plane is displayed in Table 3. The specific trajectories for the applied load moving between σ_0 and the unload state are plotted in the deviatoric plane are shown in Figure 5(a.1).

The shakedown limits derived above are found from a consideration of points on the edge of the hole only. For them to constitute a valid application of Melan's theorem, a full field comparisons of the state of stress after transient in a shake-down state, characterized by Von-Mises' parameter for all of the above cases are needed. The Von-Mises' stress is represented by the following equation in the plane stress condition:

$$\sigma_v=\sqrt{\sigma_{rr}^2+\sigma_{\theta\theta}^2-\sigma_{rr}\sigma_{\theta\theta}+3\sigma_{r\theta}^2}. \tag{14}$$

It was firstly found that the critical points did indeed always lie on the surface of the hole. Example cases of the states of stress at what were judged to be the critical-points in the loading cycle are shown in Figure 6. Again, we take $n=0$ as an typical example to represent the stress state behavior at critical points when $-1\le n\le 1/3$, shown in Figure 6(a) (applied load $\sigma_0=\lambda k$) and (b) (unload state). The above figures demonstrate that two critical locations are $(a,0)$ and $(a,\pi/2)$, and those points reach the yielding surface at maximum applied load state, i.e., σ_0. For the case $1/3<n\le 1$, we take $n=0.5$ as an example, and the full field checks are shown in Figure 6(c) (applied load $\sigma_0=\lambda k$) and (d) (unload state). Two extremes in this case occur at the same point $(a,\pi/2)$, happen at both load and unload states. Secondly, compared with the elastic solution, i.e., equation (1), all points in the plate are within the elastic limit $\sqrt{3}k$, which indicates that shakedown limit and the auxiliary stress field derived from Melan's theorem considering only the points on the edge of the hole are valid.

Marching in Time Solution

An elastic-plastic analysis of the problem in which the applied loads are shown in Figure 1 were exerted and the response tracked out as a function of time. The problem studied was analysed using the commercial finite element programme ABAQUS. The outer boundary was set at $r/a=50$ and a carefully graded mesh was used. Convergence checks were also made assiduously. The material was assumed to have an elastic almost-perfectly plastic constitutive law with a gradient in the plastic range of $10^{-4}E$, where E is Young's modulus. The very small amount of work hardening was declared to be of the

Table 2. Magnitude of elastic stress and residual stress on the deviatoric plane for $n = 0$, when plate is loaded under the shakedown limit found by Melan's theorem, $\sigma_0/k = \sqrt{3}/2$.

Elastic stress	Magnitude	Resiudal stress	Magnitude
$\sigma_{\theta\theta}(a,0) = -\frac{\sqrt{3}}{2}k$	$\lvert\sigma_{\theta\theta}(a,0)\rvert_e = \frac{\sqrt{2}}{2}k$	$\sigma^{res}_{\theta\theta}(a) = -\frac{\sqrt{3}}{2}k$	$\lvert\sigma^{res}_{\theta\theta}(a)\rvert_e = \frac{\sqrt{2}}{2}k$
$\sigma_{\theta\theta}(a,\pi/2) = \frac{3\sqrt{3}}{2}k$	$\lvert\sigma_{\theta\theta}(a,\pi/2)\rvert_e = \frac{3\sqrt{2}}{2}k$	$\sigma^{res}_{\theta\theta}(a) = -\frac{\sqrt{3}}{2}k$	$\lvert\sigma^{res}_{\theta\theta}(a)\rvert_e = \frac{\sqrt{2}}{2}k$

Table 3. Magnitude of elastic stress and residual stress on the deviatoric plane for $n = 0.5$, when plate is loaded under the shakedown limit found by Melan's theorem

Elastic stress	Magnitude	Resiudal stress	Magnitude
$\sigma_{\theta\theta}(a,0) = -\frac{2\sqrt{3}}{5}k$	$\lvert\sigma_{\theta\theta}(a,0)\rvert_e = \frac{2\sqrt{2}}{5}k$	$\sigma^{res}_{\theta\theta}(a) = -\sqrt{3}k$	$\lvert\sigma^{res}_{\theta\theta}(a)\rvert_e = \sqrt{2}k$
$\sigma_{\theta\theta}(a,\pi/2) = 2\sqrt{3}k$	$\lvert\sigma_{\theta\theta}(a,\pi/2)\rvert_e = 2\sqrt{2}k$	$\sigma^{res}_{\theta\theta}(a) = -\sqrt{3}k$	$\lvert\sigma^{res}_{\theta\theta}(a)\rvert_e = \sqrt{2}k$

kinematic type . Loads were applied in ten steps and after the first cycle of load, all subsequent turning points were chosen to be at 95% of the initial value in order to avoid ambiguities which arise when a region is on the verge of entering the plastic state. The shakedown limits implied by the calculations described in §3.1 were probed by carefully advancing the range of load until cyclic plasticity was detected.

The shakedown limit found from FEA is shown in Figure 2(a) as the red line. Notice that the numerical values from FEA were consistent with that implied by Melan's theorem when the critical locations occur at the same point of both forward and reverse direction, i.e.,

$$\lambda = \frac{2\sqrt{3}}{3-n} = 2\sigma_E. \tag{15}$$

It is found that for the range $1/3 < n \leq 1$, the actual shakedown limit coincides with that found by Melan's theorem.

The reason that the lower bound results cannot track the actual shakedown limit when $-1 \leq n < 1/3$, is that the actual residual stress can change with the value of θ to eliminate the effect on the shakedown limit from other different points expect $(a,\pi/2)$. Therefore, the actual shakedown limit calculation would focus only on the extremes produced by the point with severest stress state, i.e., $(a,\pi/2)$. But the axi-symmetrical auxiliary stress field always provides same residual stress in every different value of θ. Hence, when shakedown limits were calculated using the lower bound theorem, we need to consider the possibility that the auxiliary stress might result in the reverse direction plasticity at other different θs. The typical example would be the pure shear case, i.e., $n = -1$. The comparison between the axi-symmetrical residual stress implied by Melan's theorem when the lower bound shakedown limit applies, and the actual residual stress implied by the actual shakedown limit was plotted with respect to the values of θ, for points on the edge of the hole, indicated in Figure 2(b). In this case, no beneficial residual stress available from Melan's theorem because the axi-symmetrical residual stress is unable to deal with the situation that stress states at $(a, 0)$ and $(a, \pi/2)$ reach the elastic limit in both directions. The actual residual stress, however, can change with value of θ from negative elastic limit to positive elastic limit, hence it eliminates the effect of the reversed direction plasticity brought by points around $\theta = 0$ and then give the shakedown limit twice as that derived from Melan's theorem.

We will further illustrate that by comparing the stress trajectories at two controlling points in the deviatoric plane for the actual case and the case implied by Melan's theorem, again, for $n = 0$ and $n = 0.5$ respectively. Firstly, for $n = 0$, where the shakedown limit in the actual case is higher than that derived from Melan's theorem, in the actual case the magnitude of relevant stress on the deviatoric plane when the plate is subjected to the actual shakedown limit (point S in Figure 2(a)) are shown in Table 4, also the corresponding trajectories are shown in Figure 4(a.2). Additionally, when the plate is loaded under the shakedown limit implied by Melan's theorem and the actual shakedown limit, the specific comparison between the corresponding residual stress on the edge of the hole with respect to θ is shown in figure 4(b). From both figures, in the actual case, residual stress varies from $(a, 0)$ to $(a, \pi/2)$, which enable larger shakedown limit to be obtained for $n = 0$.

Secondly, for the case $n = 0.5$, the actual shakedown limit coincides with that derived from Melan's theorem. The same as above, when plates are loaded under the corresponding shakedown limit, the magnitude of relevant stress on the deviatoric plane in the actual loading case (point Q in Figure 2(a)), are shown in Table 5. Additionally, the deviatoric stress trajectories for a load-unload cycle together with the relevant residual stress comparison on the edge of the hole are displayed in Figure 5(a.2) and Figure 5(b). Even though from the above two diagrams, the residual stresses are different at two controlling points in the actual case, but stress arose at other points except $(a, \pi/2)$ does not consider as the extreme stress state. It was found that, for the case $1/3 < n \leq 1$, both lower bound shakedown limit and the actual shakedown limit implied that two extremes of the loading cycle occur at the same point, $(a, \pi/2)$, and this also explained the coincidence of the two corresponding shakedown limits when $1/3 < n \leq 1$.

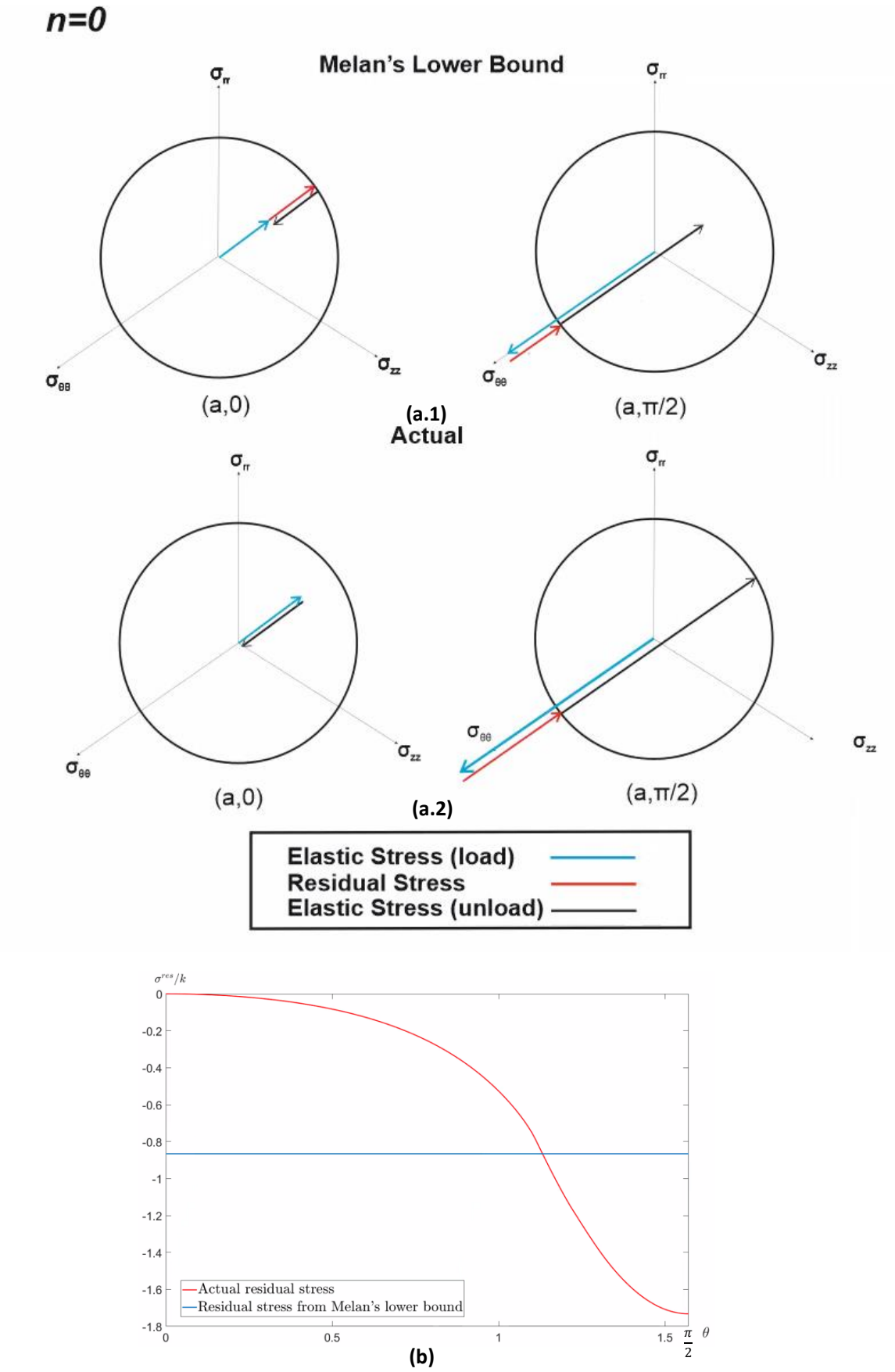

Figure 4. Load-unload case, $n = 0$, when the applied load moves between an unloaded state and $\sigma_0 = \lambda k$: (a.1) Elastic stress, residual stress in the deviatoric plane for Melan's lower bound. (a.2) Elastic stress, residual stress in the deviatoric plane for the actual case. (b) Comparison between the residual stress field at the edge of the hole in both actual and lower bound case, at different degree θ.

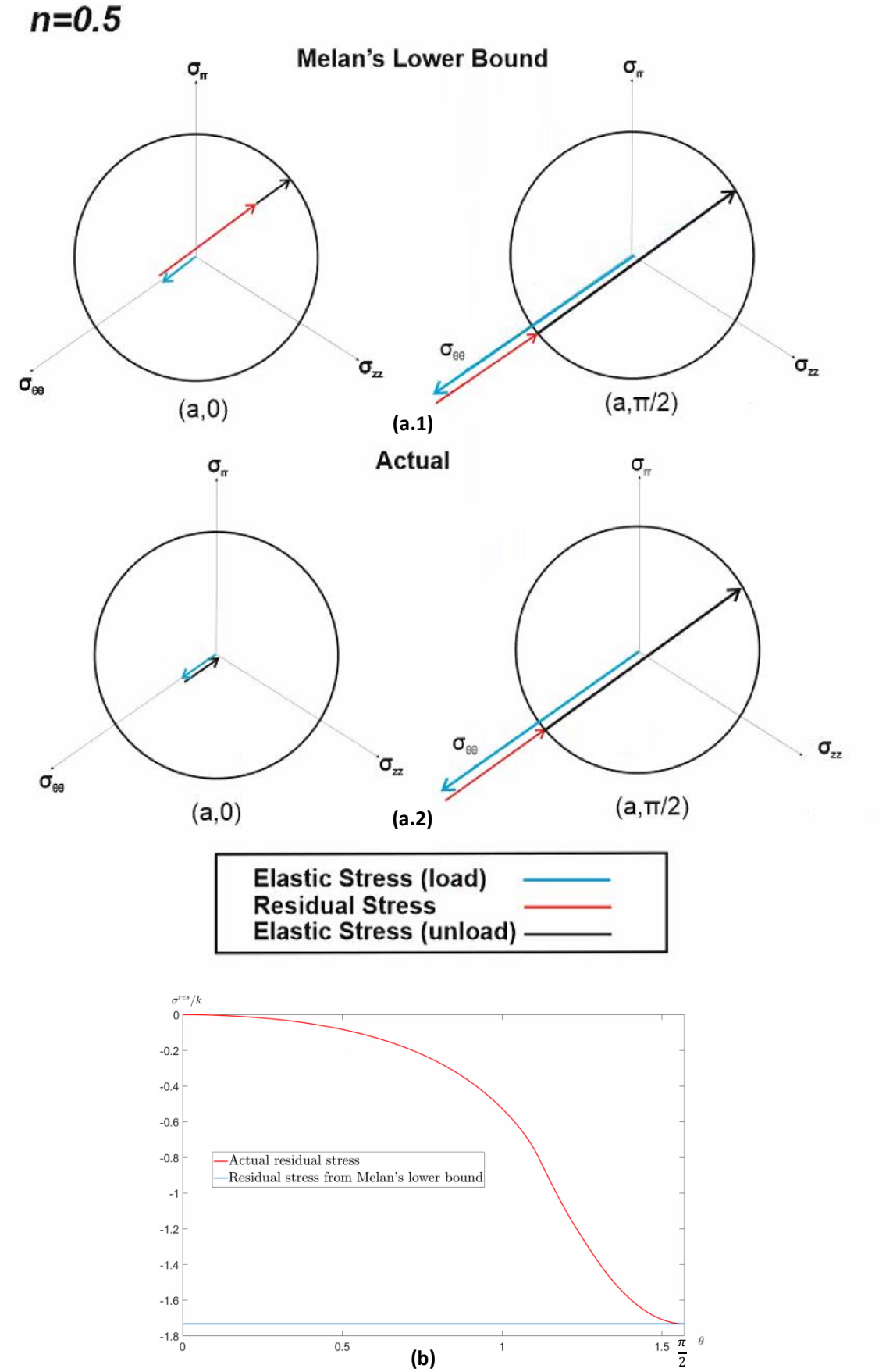

Figure 5. Load-unload case, $n = 0.5$, when the applied load moves between an unloaded state and $\sigma_0 = \lambda k$: (a.1) Elastic stress, residual stress in the deviatoric plane for Melan's lower bound. (a.2) Elastic stress, residual stress in the deviatoric plane for the actual case. (b) Comparison between the residual stress field at the edge of the hole in both actual and lower bound case, at different degree θ.

Table 4. Magnitude of elastic stress and residual stress on the deviatoric plane for $n = 0$, when plate is loaded under the actual shakedown limit.

Elastic stress	Magnitude	Resiudal stress	Magnitude
$\sigma_{\theta\theta}(a,0) = -\frac{2\sqrt{3}}{3}k$	$\lvert\sigma_{\theta\theta}(a,0)\rvert_e = \frac{2\sqrt{2}}{3}k$	$\sigma^{res}_{\theta\theta}(a,0) = 0$	$\lvert\sigma^{res}_{\theta\theta}(a,0)\rvert_e = 0$
$\sigma_{\theta\theta}(a,\pi/2) = 2\sqrt{3}k$	$\lvert\sigma_{\theta\theta}(a,\pi/2)\rvert_e = 2\sqrt{2}k$	$\sigma^{res}_{\theta\theta}(a,\pi/2) = -\sqrt{3}k$	$\lvert\sigma^{res}_{\theta\theta}(a,\pi/2)\rvert_e = \sqrt{2}k$

Table 5. Magnitude of elastic stress and residual stress on the deviatoric plane for $n = 0.5$, when plate is loaded under the actual shakedown limit.

Elastic stress	Magnitude	Resiudal stress	Magnitude
$\sigma_{\theta\theta}(a,0) = -\frac{2\sqrt{3}}{5}k$	$\lvert\sigma_{\theta\theta}(a,0)\rvert_e = \frac{2\sqrt{2}}{5}k$	$\sigma^{res}_{\theta\theta}(a,0) = 0$	$\lvert\sigma^{res}_{\theta\theta}(a,0)\rvert_e = 0$
$\sigma_{\theta\theta}(a,\pi/2) = 2\sqrt{3}k$	$\lvert\sigma_{\theta\theta}(a,\pi/2)\rvert_e = 2\sqrt{2}k$	$\sigma^{res}_{\theta\theta}(a,\pi/2) = -\sqrt{3}k$	$\lvert\sigma^{res}_{\theta\theta}(a,\pi/2)\rvert_e = \sqrt{2}k$

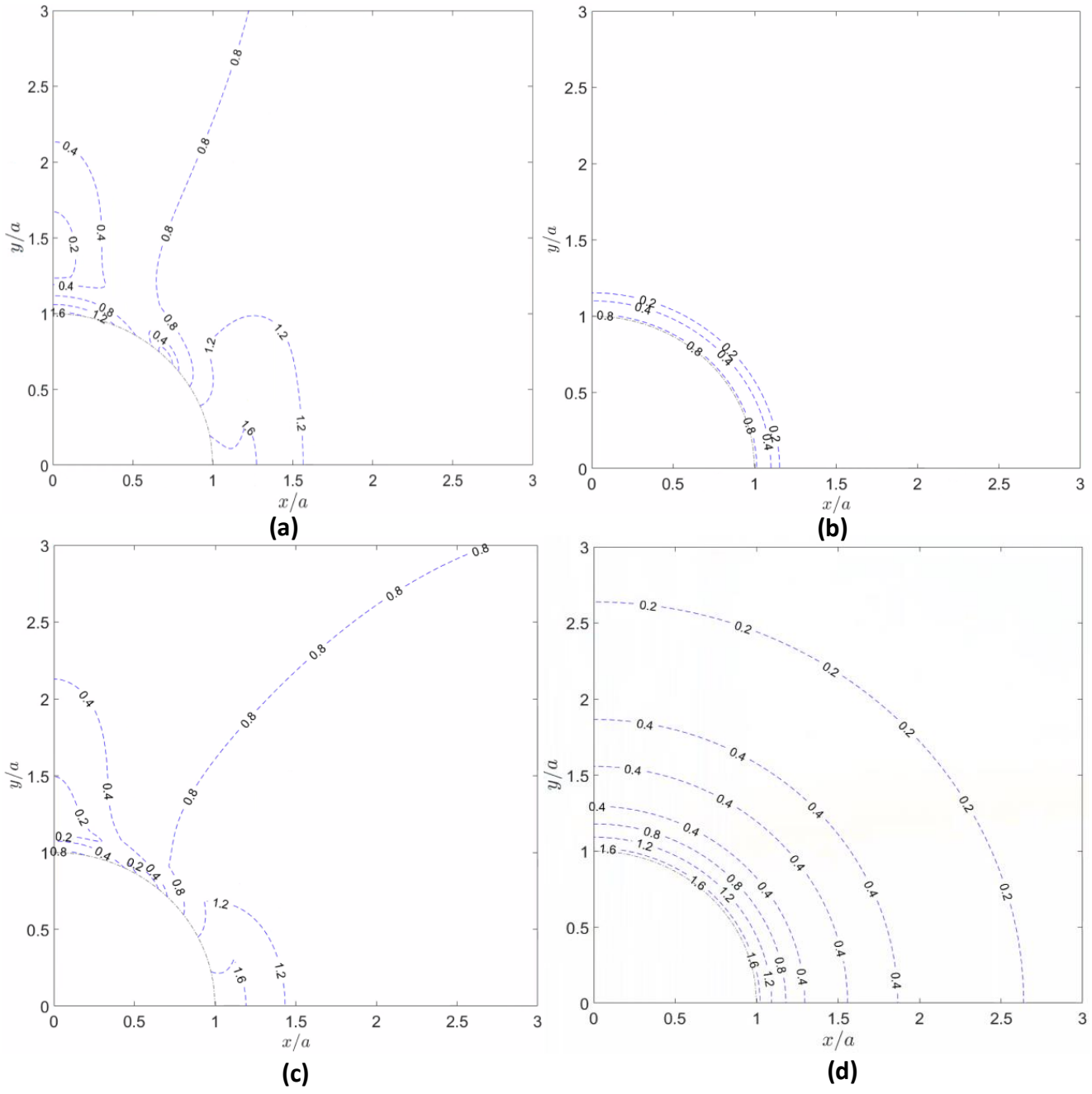

Figure 6. State of stress (σ_v/k) after transient in a shake-down state (applied load moving between an unloaded state and $\sigma_0 = \lambda k$): (a) applied load $\sigma_0 = \lambda k$, $n = 0$, (b) the unload state, $n = 0$, (c) applied load $\sigma_0 = \lambda k$, $n = 0.5$, (d) the unload state, $n = 0.5$.

Varying Degrees of Load Reversal

The last example looked at in §3 demonstrates that it is not just the state of stress at maximum applied load which matters, but also that at the opposite end of the loading cycle. The problems looked at so far have an applied load which implicitly varies between zero and σ_0, but in some cases the applied load may vary over a different range, say between $m\sigma_0$ and σ_0, where $-1 < m < 1$, so we will extend our considerations in §3 to more general cases, defined in (m, n) space, where each varies over the interval $[-1\ 1]$. First, note that when the applied load is fully reversing ($m = -1$) the state of applied stress fully reverses at every point, so that no residual state of stress can be beneficial.

Consider, next, a uniaxial state of stress ($n = 0$), same as the above, there are two key controlling points in physical space, $(a, 0)$ and $(a, \pi/2)$, and two extremes of load range σ_0 and $m\sigma_0$ to consider. Hence, there will be totally four combinations that can be considered as possible conditions for load extremes. The net state of stress at these four conditions are displayed in Table 6. Therefore, by applying Melan's theorem with axi-symmetrical auxillary stress, in choosing an optimal residual stress field we are looking for the value of $\sigma^{res}_{\theta\theta}$ which minimises the absolute difference between any pair of entries in Table 6. We know, from reasoning in the last section, that when $m = 0$ (and presumably, close to zero) the biggest difference is between entries (2,1) and (2,2) in Table 6, and this continues to hold until $m < -1/3$. Otherwise the limitation is between entries (1,2) and (2,2), and in this case we have that the optimal value for the residual stress is given by

$$2\sigma^{res}_{\theta\theta} = -3\sigma_0\,(m+1)\,,$$

which gives a shakedown limit of $\sigma_0/k = 2\sqrt{3}/(3-3m) = 2\sigma_E/(1-m)$, where σ_E is the elastic limit.

Table 6. value of $\sigma_{\theta\theta}(a,\theta)$ at $\theta = 0$ and $\theta = \pi/2$ at two load extremes, for a uniaxial load ($n = 0$), when the applied load moves between σ_0 and $m\sigma_0$.

	$\theta = 0$	$\theta = \pi/2$
$m\sigma_0$	$-m\sigma_0 + \sigma^{res}_{\theta\theta}(a)$	$3m\sigma_0 + \sigma^{res}_{\theta\theta}$
σ_0	$-\sigma_0 + \sigma^{res}_{\theta\theta}$	$3\sigma_0 + \sigma^{res}_{\theta\theta}$

We now extend this reasoning to the case where both the remote loading is more general in character and the degree of load reversal is itself a parameter. The table just introduced now needs to be extended to include n in the general case. The net state of stress at load extremes for the general case is shown in Table 7.

Table 7. value of $\sigma_{\theta\theta}(a,\theta)$ at $\theta = 0$ and $\theta = \pi/2$ at load extremes, for general load combinations, when the applied load moves between σ_0 and $m\sigma_0$.

	$\theta = 0$	$\theta = \pi/2$
$m\sigma_0$	$\sigma_0 m\,(3n-1) + \sigma^{res}_{\theta\theta}$	$\sigma_0 m(3-n) + \sigma^{res}_{\theta\theta}$
σ_0	$\sigma_0\,(3n-1) + \sigma^{res}_{\theta\theta}$	$\sigma_0\,(3-n) + \sigma^{res}_{\theta\theta}$

When $n \le 1/3$, which includes the case of uniaxial loading, $n = 0$, treated above, the biggest difference is between the entries (2,1) and (2,2) in Table 7, if $(3n-1)/(3-n) \le m < 1$, otherwise it is between entries (1,2) and (2,2). Hence the optimal residual stress are:

$$-1 \le n \le 1/3 \begin{cases} 2\sigma^{res}_{\theta\theta} = -\sigma_0\,(m+1)\,(3-n), \\ \qquad\qquad -1 \le m \le \frac{3n-1}{3-n}; \\ 2\sigma^{res}_{\theta\theta} = -2\sigma_0(1+n), \\ \qquad\qquad \frac{3n-1}{3-n} < m \le 1 \end{cases} \tag{16}$$

and the corresponding shakedown limits $\sigma_0/k = \lambda$ are:

$$-1 \le n \le 1/3 \quad \begin{cases} \lambda = \frac{2\sqrt{3}}{(3-n)(1-m)} = \frac{2}{1-m}\sigma_E, \\ \qquad\qquad -1 \le m \le \frac{3n-1}{3-n}; \\ \lambda = \frac{\sqrt{3}}{2-2n}, \\ \qquad\qquad \frac{3n-1}{3-n} < m \le 1. \end{cases} \tag{17}$$

When $n > 1/3$, for $m < 0$ the extremes of the stress state in the loading cycle occur at the same point, i.e., at $(a,\pi/2)$, hence the biggest difference is between entries (1,2) and (2,2). physically when $m > 0$, we notice that at both external extremes, $(\sigma_0,\ m\sigma_0)$, the stress state at $\theta = 0$ has the same sign as that at $\theta = \pi/2$ but is of smaller magnitude. Therefore, the biggest difference is between entries (1,1) and (2,2). The optimal residual stress are:

$$1/3 < n \le 1 \quad \begin{cases} 2\sigma^{res}_{\theta\theta} = -\sigma_0\,(m+1)\,(3-n), \\ \qquad\qquad -1 \le m \le 0; \\ 2\sigma^{res}_{\theta\theta} = \frac{n-3}{3-n+3mn-m}\sigma_0, \\ \qquad\qquad 0 < m \le 1. \end{cases} \tag{18}$$

and the corresponding shakedown limits are:

$$1/3 < n \le 1 \quad \begin{cases} \lambda = \frac{2\sqrt{3}}{(3-n)(1-m)} = \frac{2}{1-m}\sigma_E, \\ \qquad\qquad -1 \le m \le 0; \\ \lambda = \frac{2\sqrt{3}}{3-n-3mn+m}, \\ \qquad\qquad 0 < m \le 1. \end{cases} \tag{19}$$

Notice that when (m,n) is (1,1), the shakedown limit was calculated as $\lambda = \infty$. However, in elastic perfectly plastic material, stress included secondary stress is bounded by the elastic limit. Therefore, the external load of σ_0 is limited by the following inequality:

$$\sigma_0(3n-1) - \sqrt{3}k \le \sqrt{3}k, \tag{20}$$

or $\lambda \le \frac{2\sqrt{3}}{3-n}$ which is smaller than $\frac{2\sqrt{3}}{3-n-3mn+m}$ for the range $1/3 < n \le 1$ and $0 < m \le 1$. And when (m,n) lies in this range, failure will be resulted by the secondary plastic strain instead of by the accumulated plastic strain. To summarize the above, the limitations of the external load for $1/3 < n \le$

1 are:

$$1/3 < n \leq 1 \quad \begin{cases} \lambda = \frac{2\sqrt{3}}{(3-n)(1-m)} = \frac{2}{1-m}\sigma_E, & -1 \leq m \leq 0; \\ \lambda = \frac{2\sqrt{3}}{3-n}, & 0 < m \leq 1. \end{cases} \tag{21}$$

The contour plot of shakedown limits or applied load limits normalized by k, is shown in Figure 7(a) according to equations (17) and (21). Values of λ for special cases (Pure Shear, Uniaxial Load and Cylindrical load) are shown in Figure 7(b) with respect to m.

Apart from the above analysis using Melan's theorem, We also extend our FEA to the full (m,n) space. Firstly, for the range of m from -1 to 0, which includes the case we analysed in §3, the numerical value of the shakedown limit proved to be consistent with

$$\lambda = \frac{2\sqrt{3}}{(3-n)(1-m)} = \frac{2}{1-m}\sigma_E. \tag{22}$$

Notice that this is the shakedown limit calculated by using entries (1,2) and (2,2) in Table 7. And again this implies that in the actual case, two extremes of the loading cycle occur at the same point, hence the reason that explained under a certain range of n, lower bound shakedown limit is unable to track the actual shakedown limit in §3 still holds. In other words, the coincidence between the shakedown limit in the actual case and that derived from Melan's theorem happens when two extremes during the cyclic loading occur at the same point. The range for the above coincidence happening is characterized by the first range of (m,n) in equation (17) and equation (21), i.e., $-1 \leq n \leq 1/3$ and $-1 \leq m \leq \frac{3n-1}{3-n}$; $1/3 < n \leq 1$ and $-1 \leq m \leq 1$, the above also can be rewritten as $-1 \leq m \leq 0$ and $n \geq \frac{3m+1}{3+m}$.

We need to be aware of the secondary plastic flow when considering the case $0 < m \leq 1$. As mentioned above, in this case, equation (21) does not continually provide the shakedown limit because the residual stress implied at $(a, \pi/2)$ is larger than the elastic limit for $0 \leq m \leq 1$ when $0 < m \leq 1$. Therefore the maximum external load will be the shakedown limit implied by equation (20),

$$\lambda = \frac{2\sqrt{3}}{3-n}. \tag{23}$$

The maximum loads found from FEA are consistent with equation (23) by showing non-convergency at some internal points when the applied load is equal or greater than that indicated in equation (22), and no accumulated plastic strain when the applied load is below that value. Therefore, for $0 < m \leq 1$, lower bound theorem can successfully calculate the actual shakedown limit when the axi-symmetrical residual stress at the edge of the hole equals to the elastic limit in the reversed direction, i.e., $-\sqrt{3}k$, which happens in the range $1/3 < n \leq 1$, indicated in equation (20).

To summarize the above, from FEA, the estimated actual shakedown limits are the following for the full (m,n) space:

$$\begin{cases} \lambda^{actual} = \frac{2\sqrt{3}}{(3-n)(1-m)} = \frac{2}{1-m}\sigma_E, & -1 \leq m \leq 0; \\ \lambda^{actual} = \frac{2\sqrt{3}}{3-n}, & 0 < m \leq 1. \end{cases} \tag{24}$$

the above have been plotted in contours, in Figure 8(a). Additionally, the comparison between the actual shakedown/applied load limits and those calculated by Melan's lower bound, represented by the difference $e = (\lambda^{actual} - \lambda)/\lambda^{actual}$, is shown in Figure 8(b). The space of the coincidence is:

$$\{-1 \leq m \leq 0, n \geq \frac{3m+1}{3+m}\} \cup \{0 < m \leq 1, n \geq 1/3\}. \tag{25}$$

This space was indicated as the region marked by '$e = 0$'. Lastly, from the diagram, we can conclude that for the entire range of m, the shakedown limits produced by Melan's lower bound are getting closer to the exact solution with the increase of the value of n.

Conclusion

The paper provides valuable insight into the implementation of Melan's lower bound shakedown theorem applied to an accessible problem, viz. a circular hole in an infinite plate subject to an arbitrary remote stress. The often practically encountered limiting factors arising in what is essentially a "min-max" problem - finding the maximum value of the state of stress over the load cycle, and choosing the optimal residual stress state to achieve it - is done in way which minimises the amount of mathematics needed.

The shakedown limit calculated by Melan's theorem is shown in equations (17) and (21), also indicated in Figure 7; and the actual shakedown limit predicted by FEA is shown in equation (24), plotted in Figure 8. In all the cases, the actual shakedown limit implies that the extremes of the loading cycle occur at the same point, $(a, \pi/2)$, so when the shakedown limit calculated using Melan's theorem implies the same, Melan's theorem can succesfully predict the actual shakedown limit. The range of the coincidence between the lower bound shakedown limit and the actual shakedown limit is characterized by equation (25).

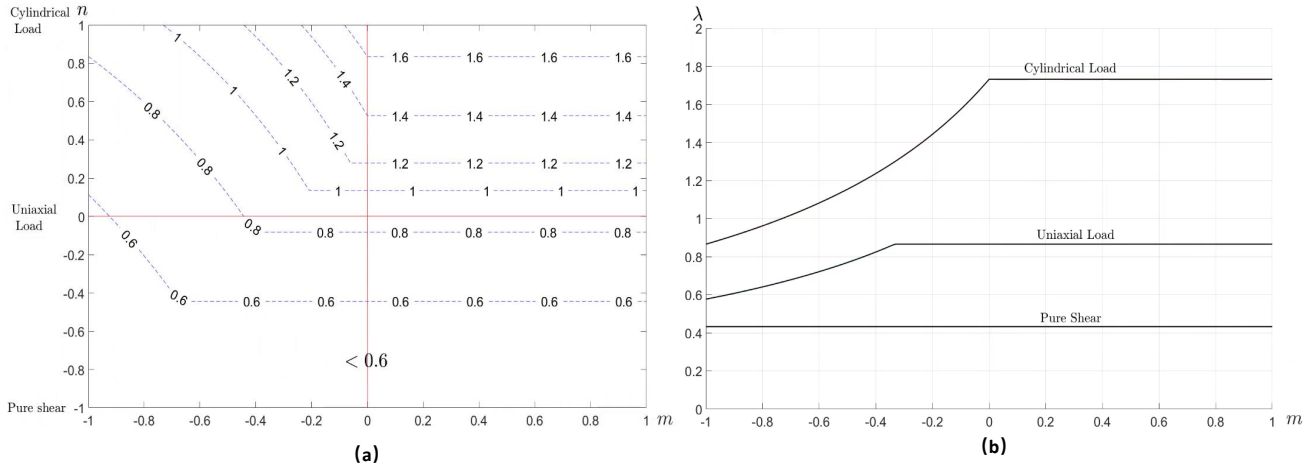

Figure 7. Values of normalized shakedown/external load limits (λ) derived from Melan's theorem: (a) Contour plot of full (m,n) space, (b) For special cases, pure shear ($n = -1$), uniaxial Load ($n = 0$) and Cylindrical Load ($n = 1$).

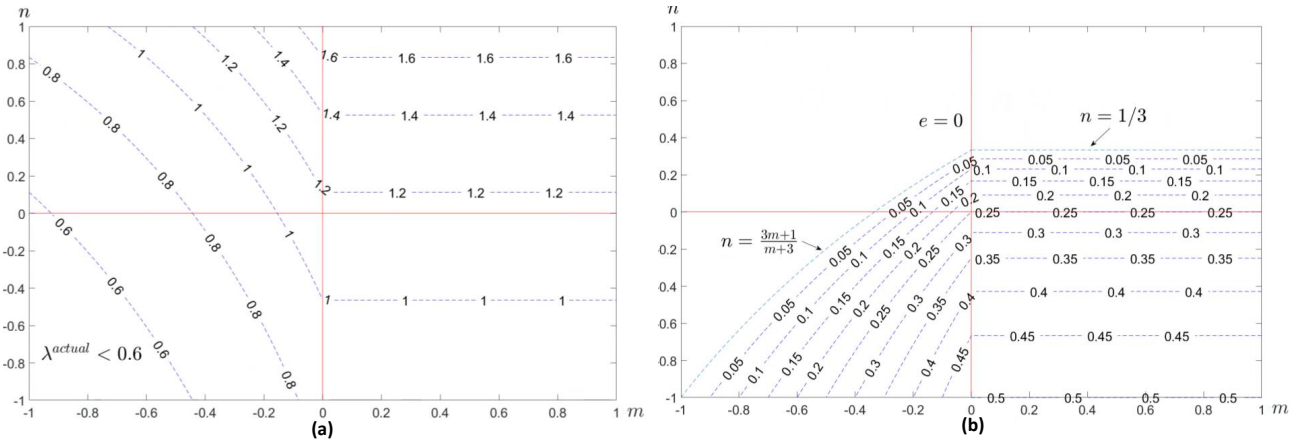

Figure 8. (a) Values of actual shakedown/external load limits (λ^{actual}) derived from a finite element model, (b) Values of the difference e between the shakedown/external load limits found by Melan's lower bound and the actual shakedown limits.

References

1. **Bleich H**. Über die Bemessung statisch unbestimmter Stahltragwerke unter Berücksichtigung des elastisch-plastischen Verhaltens des Baustoffes. *Bauingenieur*; 1932 19(20): 261-266
2. **Bleich F. and Melan E.** Die gewöhnlichen und partiellen Differenzengleichungen der Baustatik. *Springer-Verlag*; 2013
3. **Koiter W.** A new general theorem on shakedown of elastic-plastic structures. *Proc. Koninkl. Ned. Akad. Wet. B*; 1956 59:23-34
4. **König J.** Shakedown of elastic-plastic structures. *Elsevier*; 2012
5. **Hamilton, R., Boyle, J. T., Shi, J. and Mackenzie, D.** Shakedown load bounds by elastic finite element analysis. *In Proceedings of ASME Conference on Pressure Vessels and Piping*, 1996, Vol. 343 (American Society of Mechanical Engineers, New York)
6. **Fushi P., Pisano A. and Aurora A. et al.** Direct methods for limit and shakedown analysis of structures. *Springer*; 2015
7. **Muscat M., Hamilton R. and Boyle J.** Shakedown analysis for Complex loading using superposition. *Journal of Strain Analysis*; 2002 37(5): 399-411
8. **Polizzotto C.** On the conditions to prevent plastic shakedown of structures: Part I—Theory. *Journal of Applied Mechanics*; 1993 60(1): 15-19
9. **Melan E.** Der Spannungszustand eines Mises-Henckys chen Kontinuums bei veraderlicher Belastung. *itzber Akad. Wiss. Wien Iia*; 1983 147: 73-78
10. **Barber J.** Elasticity *Springer*; 2002